Decay studies of ^{59}Cu* formed in the ^{35}Cl + ^{24}Mg reaction using the dynamical cluster-decay model

C. Karthikraj and M. Balasubramaniam*
Department of Physics, Bharathiar University, Coimbatore 641046, India
(Received 8 September 2012; revised manuscript received 9 November 2012; published 22 February 2013)

The reformulated dynamical cluster-decay model (DCM) is applied to study the decay of odd-A and non-α structured ^{59}Cu* formed in the ^{35}Cl + ^{24}Mg reaction at $E_{\rm lab} = 275$ MeV. Here, the temperature (T)–dependent binding energies due to Krappe are used. The roles of Wigner and pairing energies in the fragmentation potential are explicitly shown in this work. For the temperature $T = 4.1898$ MeV corresponding to $E_{\rm lab} = 275$ MeV, the contribution of pairing vanishes and the resulting structure of the fragmentation potential due to Wigner term is shown. In addition to this, we have studied the role of factor α appearing in the inertia part of the equation of motion dictating the mass-transfer process. It is shown that this factor has significant effect in the structure of preformation probability values and hence in turn we see significant changes in the cross sections. We compare the cross sections of the measured charge distributions of the fission fragments for two limiting values of the parameter α with the experimental data. In order to fit the total cross-section values, a linear relation is obtained between the free parameter of the model $\triangle R$ and the factor α appearing in the hydrodynamical mass.

DOI: 10.1103/PhysRevC.87.024608 PACS number(s): 25.70.Jj, 23.70.+j, 24.10.−i, 21.10.Dr

I. INTRODUCTION

The compound nuclei (CN) formed in the mass region $40 \leqslant A_{\rm CN} \leqslant 80$ in low-energy reactions have been studied extensively [1]. In these fusion-fission reactions, in addition to the light-particle evaporation, these systems possess considerable fission components. Theoretically, the de-excitation of the CN through the emission of light particles (LPs) with $A \leqslant 4$ and $Z \leqslant 2$ (n, p, α) and/or γ radiation as well as the intermediate-mass fragments (IMFs) or complex fragments have been studied using various models in the past three decades [2–10]. For an equilibrated CN, a nonstatistical description, the so-called dynamical cluster-decay model (DCM) was recently developed by Gupta and collaborators. Within this model, the decay of light, medium, heavy, and superheavy compound nuclei are studied successfully, explaining different observables from several low-energy reactions [11–24]. However, the DCM has not been applied so far to study the odd-A, non-α, light-mass CN formed in low-energy reactions.

Experimentally, the odd-A, non-α compound systems such as ^{47}V, ^{49}V, and ^{59}Cu formed in different entrance channels like ^{35}Cl + ^{12}C, ^{31}P + ^{16}O, ^{23}Na + ^{24}Mg, ^{37}Cl + ^{12}C, and ^{35}Cl + ^{24}Mg have been studied extensively at different incident energies [25–29]. Further, it has been shown that the entrance channel does not play a significant role in binary fission for the decay of ^{47}V* formed from different asymmetric ^{35}Cl + ^{12}C and ^{31}P + ^{16}O and nearly symmetric ^{23}Na + ^{24}Mg reactions at comparable excitation energies [25,26] as well as in the decay of even-A and α-structured ^{48}Cr* formed in three different incident channels [30,31]. However, for ^{59}Cu* formed in the asymmetric and nearly symmetric reactions, viz., ^{19}F + ^{40}Ca and ^{32}S + ^{27}Al, due to the onset of incomplete fusion, the measured excitation functions of fusion-like evaporation residues for the asymmetric entrance channel are shown to exceed with respect to nearly symmetric entrance channel by up to 44% [32].

Experimentally, the ^{35}Cl + ^{24}Mg → ^{59}Cu* reaction has been studied at two incident energies at $E_{\rm lab} = 275$ and 282.4 MeV [28,29]. In the reaction corresponding to $E_{\rm lab} =$ 275 MeV, the observed total evaporation residue (ER) cross sections and fission fragment (FF) cross sections are reported as 722 ± 197 and 137 ± 5 mb respectively. In this experiment, the charge distribution of the fragment cross sections are measured, and for the charges $Z = 3$ to 4 and 13 to 15, the fragment cross sections are not observed due to the mixing of large deep inelastic components. However, this difficulty has been overcome by Cavallaro *et al.* [29] for the same reaction but at an incident energy of $E_{\rm lab} = 282.4$ MeV. In this experiment, the measured ER and FF cross sections are reported respectively as 660 ± 110 and 168 ± 30 mb. Further it has been concluded that the ternary processes from these reactions are not possible, at least for the incident energies lower than that of 10 MeV/A.

Recently, the dynamical cluster-decay model has been reformulated by us [33] to study the role of one of the main ingredient of the model, namely, the use of different temperature-dependent binding energies [34,35]. It is concluded from this study that the refitting of the coefficients of the original forms of the binding energy formula are not required and the structural effects resulting in fragmentation potentials and hence in turn in the preformation probabilities and cross sections are the inherent property of the binding energy form one uses.

With the proper inclusion of temperature-dependent Wigner and pairing energies, the fully T-dependent reformulated DCM is applied in this work for the first time to study the de-excitation of the odd-A, non-α CN ^{59}Cu*, formed in the ^{35}Cl + ^{24}Mg reaction with an excitation energy of $E^*_{\rm CN} \approx$ 125 MeV corresponding to the entrance channel energy of $E_{\rm lab} = 275$ MeV.

The paper is organized as follows: The DCM is very briefly explained in Sec. II. Results obtained from the decay of odd-A

*m.balou@gmail.com

and non-α ^{59}Cu* formed in the reaction ^{35}Cl + ^{24}Mg at $E_{\rm lab}$ = 275 MeV are discussed in detail in Sec. III. Finally, summary of the results is presented in Sec. IV.

II. THE METHODOLOGY

The DCM stems from the preformed cluster model (PCM) for ground-state decays. The detailed description of the model can be found in Ref. [12]. In DCM, the decay cross section in terms of partial waves [13,14] is defined as

$$\sigma = \frac{\pi}{k^2}\sum_{\ell=0}^{\ell_{\max}}(2\ell+1)P_0P; \quad k=\sqrt{\frac{2\mu E_{\rm c.m.}}{\hbar^2}}, \tag{1}$$

Here, P_0 refers to the preformation probability of the emitted fragments referring to η motion and P is the penetrability referring to R motion. The preformation probabilities of the fragments are obtained by numerically solving the stationary Schrödinger equation governing the η coordinate motion, at a fixed R:

$$\left\{-\frac{\hbar^2}{2\sqrt{B_{\eta\eta}}}\frac{\partial}{\partial\eta}\frac{1}{\sqrt{B_{\eta\eta}}}\frac{\partial}{\partial\eta}+V_R(\eta,T)\right\}\psi^{\nu}(\eta)=E^{\nu}\psi^{\nu}(\eta), \tag{2}$$

with $\nu = 0, 1, 2, 3, \ldots$ referring to ground-state ($\nu = 0$) and excited-state solution. The solution to this equation after normalization gives the preformation probability as

$$P_0(A_i) = |\psi(\eta(A_i))|^2\sqrt{B_{\eta\eta}}\frac{2}{A}, \tag{3}$$

where P_0 contains the structural information of the compound nucleus which enters through the fragmentation potentials. The T-dependent fragmentation potential for the mass asymmetry coordinate η at a fixed R is given by

$$\begin{aligned}V(\eta,T,\ell) = &-\sum_{i=1}^{2}[BE_{\rm LDM}(A_i,Z_i,T)]+\sum_{i=1}^{2}\delta U_i(T)\\ &+\frac{Z_1Z_2e^2}{R(T)}+4\pi\bar{R}(T)\gamma b(T)\Phi[s(T)]\\ &+\frac{\hbar^2\ell(\ell+1)}{2I_S(T)}.\end{aligned} \tag{4}$$

The first term of this equation corresponds to the temperature-dependent binding energy of the fragments and is calculated from the expression given by Krappe in Ref. [34]. This binding energy expression contains T-dependent Wigner and pairing terms in addition to the T-dependent liquid drop proper. The second term correspond to the shell corrections, which are calculated using the analytical form of Myers and Swiatecki [37] and are considered to vanish exponentially with temperature. The pairing and shell correction terms though are important for reproducing the ground-state binding energies [see panels (b) and (c) in Fig. 1] but do not have much significance at higher excitation energies and in particular at the temperature of our interest in the present study. In general, the contributions due to pairing and shell corrections are found to vanish beyond $T \approx 2$ MeV [shown in panels (e) and (f) in Fig. 1]. However, an additional term, the so-called Wigner term, has a significant role in the mass formula in order to reproduce the kinks of the nuclear mass surface. Its effect is to decrease the binding when $N \neq Z$. Moreover, it has significant contribution at higher excitation energies as well. In other words, Wigner energy does not vanish up to $T = 4$ MeV [see panel (d) in Fig. 1]. It indeed has a significant role even at the temperature considered in this work. The other three terms correspond respectively to Coulomb potential, nuclear proximity potential, and centrifugal potential. The details of this Eq. (4) and the reformulated DCM can be found in Ref. [33]. The barrier penetration probability in Eq. (1) is calculated within WKB approximation as

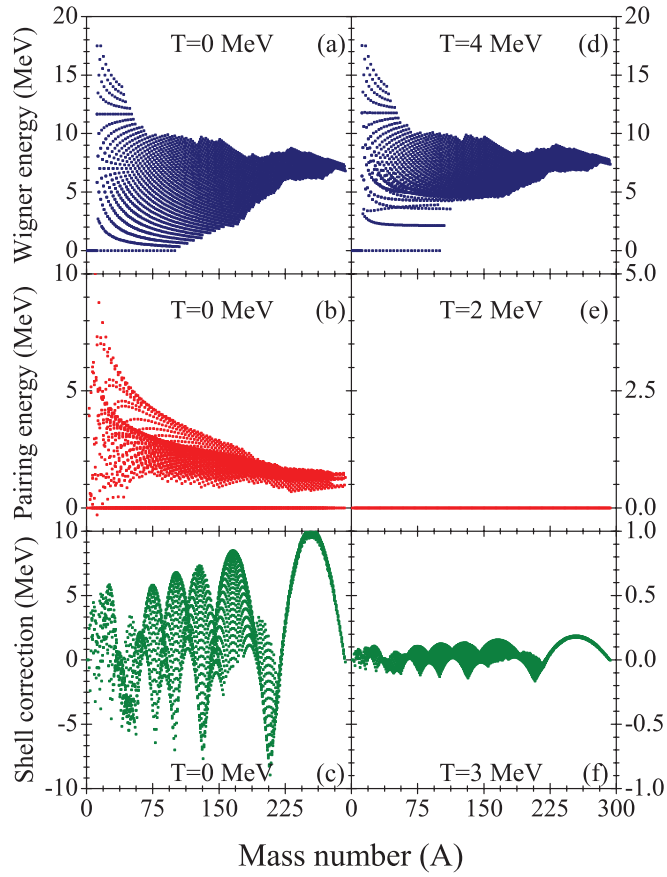

FIG. 1. (Color online) Wigner, pairing, and shell correction energies calculated at ground-state ($T = 0$ MeV) and higher temperatures for experimentally known nuclei [36].

$$P = \exp\left[-\frac{2}{\hbar}\int_{R_a}^{R_b}\{2\mu[V(R)-Q_{\rm eff}]\}^{1/2}dR\right]. \tag{5}$$

III. RESULTS AND DISCUSSION

One of the main ingredients of the DCM as mentioned earlier is the use of temperature-dependent binding energies. In the reformulated DCM, the T-dependent binding energies due to Krappe are used. It is to be mentioned here that the T-dependence is also considered in Wigner and pairing

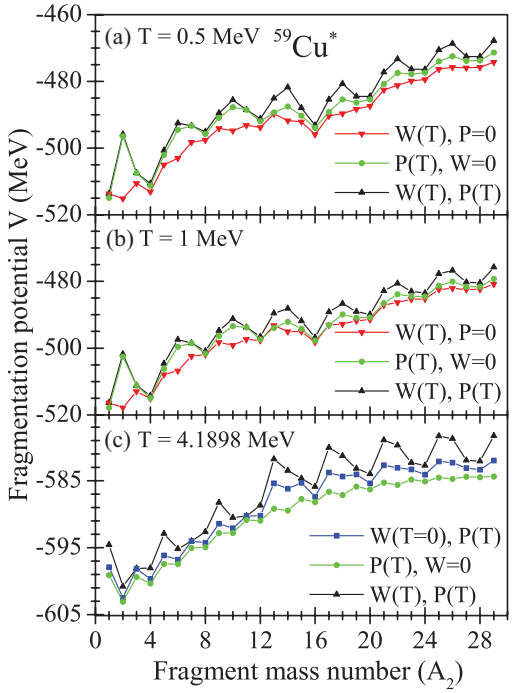

FIG. 2. (Color online) The binary fragmentation potentials for the decay of ^{59}Cu* at (a) $T = 0.5$ MeV, (b) $T = 1$ MeV, and (c) $T = 4.1898$ MeV. $W(T)$ and $P(T)$ refers to temperature-dependent Wigner and pairing terms. $W(T = 0)$ refers to the Wigner term at $T = 0$ MeV and $W = 0$, and $P = 0$ refers to taking the Wigner and pairing terms as zero.

energies are as prescribed by Krappe. To see the effects of temperature dependence of Wigner and pairing energies in the fragmentation potentials [as defined in Eq. (4) at $R = R_t$ $(= R_1 + R_2)$ fm and $\ell = 0\hbar$] for the binary fragmentation of ^{59}Cu*, we present in Fig. 2 the calculated fragmentation potentials corresponding to three different temperatures, $T =$ 0.5, 1.0, and 4.1898 MeV in panels (a), (b), and (c) respectively. In these figures, the upward-pointing triangles correspond to the use of binding energies with the inclusion of both T-dependent Wigner and pairing terms denoted as $W(T)$, $P(T)$. The solid circles correspond to the use of binding energies with the inclusion of T-dependent pairing energies, not including the Wigner term by considering it to be 0 MeV, denoted as $P(T)$, $W = 0$. The downward-pointing triangles in panels (a) and (b) correspond to the use of binding energies with the inclusion of the T-dependent Wigner term by considering the pairing contribution to be 0 MeV, denoted as $W(T)$, $P = 0$. The solid squares in panel (c) correspond to the use of binding energies with Wigner term at $T = 0$ MeV and T-dependent pairing term, denoted as $W(T = 0)$, $P(T)$. From panels (a) and (b) it is clear that when the pairing term is not included in the binding energies, strong minima for α nuclei are not seen and switching off the Wigner term and considering pairing term results in a four-nucleon structure. This structure prevails with the inclusion of both T-dependent Wigner and pairing terms. However this scenario changes at higher temperature, as presented in panel (c). The strong maxima seen in panels (a) and (b) for $4n + 2$ nuclei now appear for $4n + 1$ nuclei. Since at this temperature the pairing contribution will vanish automatically, we present another comparison by a considering Wigner term contribution at $T = 0$ MeV and T-dependent pairing, presented as solid squares. When the Wigner term is switched off and only T-dependent pairing is considered, due to the vanishing of pairing contribution at this temperature, there are no strong minima seen for α nuclei and only an odd-even effect prevails. However, if the Wigner term corresponding to $T = 0$ MeV is considered, and taking T-dependent pairing (which obviously vanishes), we see strong minima for heavy α nuclei starting from $A_2 = 16$ onward. When the Wigner term is considered to be T-dependent along with a T-dependent pairing term, the odd-even structure present for $A_2 < 12$ changes to a shallow valley of $4n$, $4n + 2$, and $4n + 3$ with strong maxima at $4n + 1$. The inclusion of the T-dependent Wigner term indeed has a strong influence in the structure of the potential.

In Fig. 3, we present the fragmentation potentials of ^{59}Cu* formed in the reaction $^{35}\mathrm{Cl} + ^{24}\mathrm{Mg}$ at $T = 4.1898$ MeV corresponding to $E_{\mathrm{lab}} = 275$ MeV at $R = R_t$ fm as a function of fragment mass number (A_2) and angular momentum ℓ values. The shallow valley in the potential corresponding to $4n$, $4n + 2$, and $4n + 3$ prevails for all the ℓ values; however, the competition of fission fragments with light particles starts around $\ell = 30\hbar$ onward, and at still higher ℓ values, the minima for fission fragments are lower than those of the LPs.

In addition to the role of Wigner and pairing terms analyzed in this work, we also present the role of another factor which enters the model via the hydrodynamical masses $B_{\eta\eta}$ of Kröger and Scheid [38], appearing in Eq. (2) in the inertia part of the equation of motion. It is defined as

$$B_{\eta\eta} = \frac{AmR^2}{4}\left[\frac{v_t(1+\beta)}{v_c(1+\delta^2)} - 1\right], \tag{6}$$

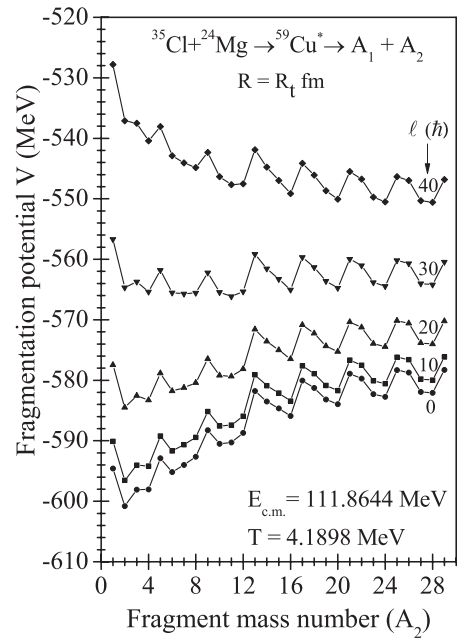

FIG. 3. The fragmentation potentials for the binary decay of ^{59}Cu* at $T = 4.1898$ MeV and $R = R_t$ fm as a function of fragment mass number (A_2) and angular momentum (ℓ).

with

$$\beta = \frac{R_c}{2R}\left[\frac{1}{1+\cos\theta_1}\left(1-\frac{R_c}{R_1}\right)+\frac{1}{1+\cos\theta_2}\left(1-\frac{R_c}{R_2}\right)\right],$$
$$\delta = \frac{1}{2R}\left[(1-\cos\theta_1)(R_1-R_c)+(1-\cos\theta_2)(R_2-R_c)\right]. \quad (7)$$

Between the two nuclear volumes of the spherical fragments, a cylinder of length R and radius R_c is assumed for the homogeneous radial mass transfer and/or flow (refer to Ref. [38] for the geometry of the model) with the volume of the cylinder $v_c = \pi R_c^2 R$ and the total conserved volume $v_t = v_1 + v_2$. For the radius of the cylinder R_c, the authors use a special ansatz:

$$R_c = \alpha \min(R_1, R_2) f\left(\frac{R}{R_t}\right) \quad (8)$$

with

$$f(x) = 1; \quad \text{if} \quad x \leqslant 1 \quad (9)$$

and

$$f(x) = \sin^2 \tfrac{1}{2}\pi x; \quad \text{if} \quad 1 \leqslant x \leqslant 2, \quad (10)$$

and α values from 0.4 to 0.8 are shown to have the best fit with the microscopic calculations [39] for the mass transfer between $^{238}\mathrm{U} + ^{238}\mathrm{U}$ with a total mass number of $A = 476$. Here, $R_t = R_1 + R_2$ defines the touching configuration, which is also equal to the length of the cylinder R. For touching and overlapping configuration $f(x)$ takes the value of 1. If R is defined to be $R_t + \triangle R$, for positive values of $\triangle R$, $f(x)$ takes the value as defined in Eq. (10). The factor α appearing in Eq. (8) has a significant effect in the calculation of preformation probabilities (P_0) as is presented in Fig. 4. This effect was recently studied by us in estimating the preformation probabilities of binary fragmentation of nuclei in different mass regions [40].

In Fig. 4, we present the calculated preformation probabilities for the use of the fragmentation potentials presented in Fig. 3 for $\ell = 0\hbar$ and $\ell = 30\hbar$ [in panels (a) and (b) respectively] corresponding to $R = R_t$ fm for the temperature $T = 4.1898$ MeV as a function of fragment mass numbers A_2 and A_1 and the factor α appearing in Eq. (9). For $\ell = 0\hbar$ in panel (a) it is clearly seen that α has nearly no role up to fragment mass numbers $A_2 = 12$ and its associated fragments A_1. However, beyond $A_2 = 12$, the preformation probability values decrease sharply for all α values, but the magnitude increases with increase in α values. For $\alpha = 0.4$, a four-nucleon transfer characteristic for nearly symmetric fragment combinations is seen which diminishes at $\alpha = 0.5$ and completely vanishes for other α values considered. However, at higher ℓ values, as presented in panel (b) for $\ell = 30\hbar$, the structure remains the same for all the α values but the pronounced maxima seen are larger for $\alpha = 0.4$ and smaller for $\alpha = 0.8$. For the other fragment combinations, the preformation values increases as α increases. The enhancement in the preformation probability values due to this factor has a significant effect in the cross-section estimates. Since the cross section is a combined effect of preformation probabilities and penetration

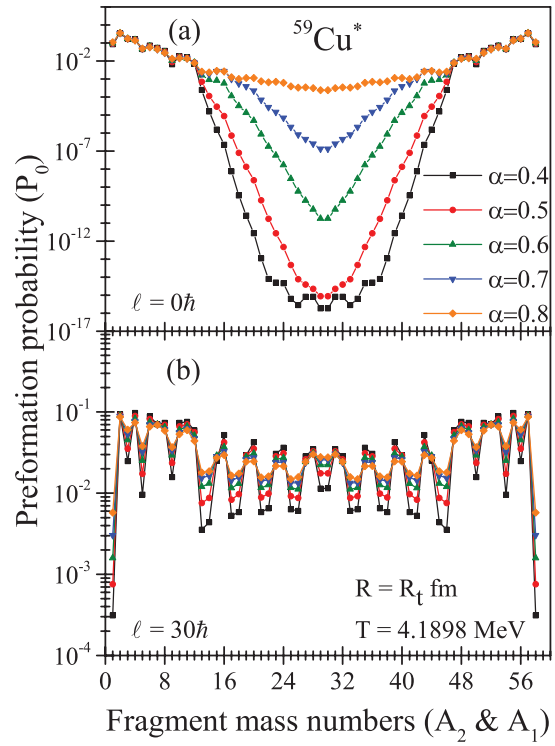

FIG. 4. (Color online) The preformation probability (P_0) for the binary decay of ^{59}Cu* at $T = 4.1898$ MeV and $R = R_t$ fm as a function of fragment mass numbers (A_1 and A_2) and the factor α. Panels (a) and (b) shows the P_0 values calculated at $\ell = 0\hbar$ and $\ell = 30\hbar$ respectively. The legend shown is the same for both panels.

probabilities, we present in Fig. 5 the summed cross sections (summed from $\ell = 0\hbar$ to $\ell_{\max}$) of all the fragments as functions of fragment mass number A_2 and α values.

In Fig. 5(a), the $\triangle R$ values (1.4453 fm for LPs and 1.3251 fm for IMFs) are obtained by fitting the experimental value of $\sigma_{\mathrm{LP}}^{\mathrm{expt.}} = 722 \pm 197$ mb and $\sigma_{\mathrm{FF}}^{\mathrm{expt.}} = 137 \pm 5$ mb (FF corresponds to fragments with charges from 5 to 12), corresponding to the use of $\alpha = 0.4$. For this $\triangle R$ and α value, our obtained results are $\sigma_{\mathrm{LP}} = 722.38$ mb, $\sigma_{\mathrm{IMF}} = 325.45$ mb (for fragments with mass numbers 5 to 29), and $\sigma_{\mathrm{FF}} = 137.05$ mb. For the same $\triangle R$, the variation of α results in the enhancement of cross section as the α value increases. However, for a fixed $\triangle R$ obtained for a particular α value, say, in this case 0.4, would not reproduce the experimental data. Hence in order to compare with the experimental data, the $\triangle R$ value has to be varied so as to obtain a better agreement with the experimental data. This result is presented in Fig. 5(b) for different values of α. In this figure, for each α value, the $\triangle R$ is obtained by fitting to the experimental data. The obtained $\triangle R$ values for different α values are presented in Fig. 6. A linear relation is also fitted for the $\triangle R$ values (for both LPs and IMFs) as a function of α as shown in the figure. The $\triangle R$ values for LPs are more or less constant but decrease with increase in α value for IMFs. For IMFs, a larger value of α requires a smaller value of $\triangle R$ and vice versa. It means if the volume of the cylinder assumed for the mass transfer is larger, the neck distance required is smaller, and vice versa.

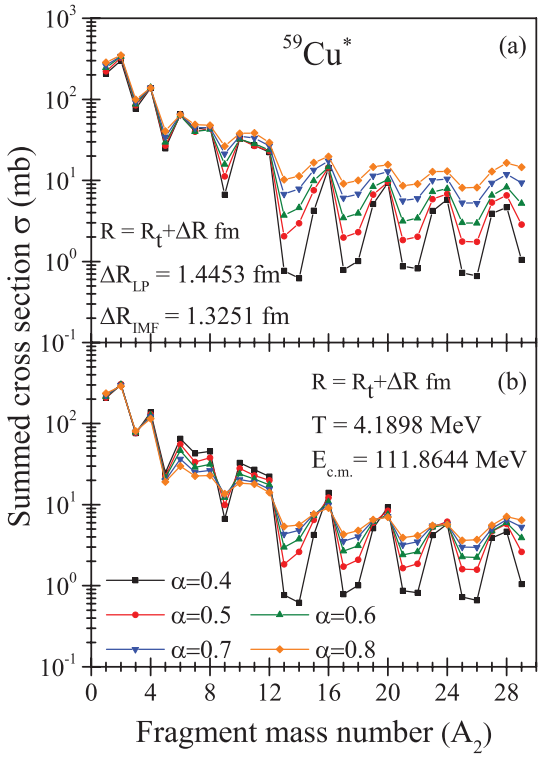

FIG. 5. (Color online) The calculated summed cross sections (from $\ell = 0\hbar$ to ℓ_{max}) for the decay of ^{59}Cu* at $T = 4.1898$ MeV and $R = R_t + \triangle R$ fm as a function of fragment mass number (A_2). Here the $\triangle R$ values in panel (a) correspond to the use of $\alpha = 0.4$ and the same $\triangle R$ is used for the other α values, and in panel (b) the $\triangle R$ values for the different α values are obtained by fitting the data. The $\triangle R$ values for the different α values are presented in Fig. 6. The legends are the same for both panels.

Finally, in Fig. 7, we present the comparison of our calculated results for the limiting cases of $\alpha = 0.4$ and 0.8, with the experimental data. For both these α values, $\triangle R$ values are different and are obtained by fitting both LP and FF cross sections. In this figure, we compare only the experimental data corresponding to the fragments with charge numbers from 5 to 12. In the calculations, while charge minimizing the potential,

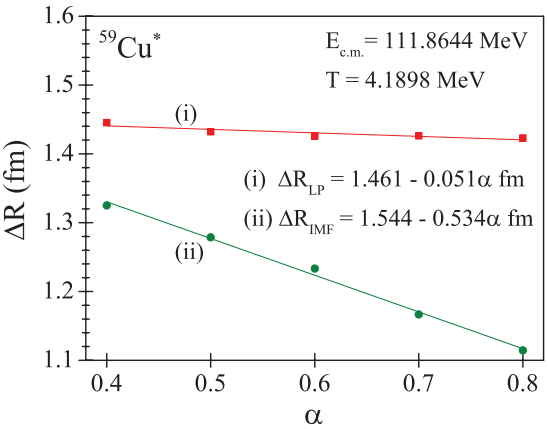

FIG. 6. (Color online) The fitted $\triangle R$ values for both the LPs and IMFs for the different α values. The fitted linear relation is also given.

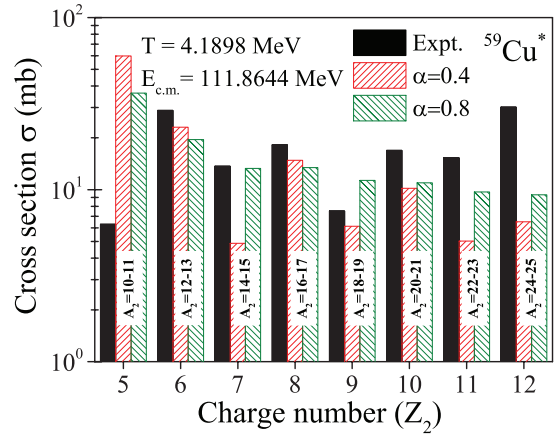

FIG. 7. (Color online) The calculated cross sections for the $\alpha = 0.4$ and 0.8 values are compared with the charge distribution of the fission fragments from the experimental data [28]. Combination of the masses shown refers to the same charge for the mentioned masses.

for the same charge there may be more mass asymmetry present. Our presented results correspond to the sum of the cross sections of the fragments possessing the same charge. For example, in the minimized potential, three fragments with mass numbers $A_2 = 9$, 10, and 11 have the charge of $Z = 5$. However, for $A_2 = 9$, the potential for the charges $Z = 4$ and 5 differ only by 0.3 MeV. Hence, we have excluded this mass in the comparison, and our results for $Z = 5$ are due to $A_2 = 10$ and 11 only. Similarly for the other charges from $Z = 6$ to 12, we have a combination of different masses as labeled in the figure. The calculated cross sections for the use of different α values differ within an order of magnitude only. The calculated results are closer to the experimental values but are not in good agreement with the experimental data.

IV. SUMMARY

To check the validity of the reformulated DCM with the T-dependent binding energy due to Krappe, we have studied the decay of odd-A and non-α ^{59}Cu* formed in the reaction ^{35}Cl + ^{24}Mg at $E_{lab} = 275$ MeV corresponding to the temperature $T = 4.1898$ MeV. The effect of T-dependent Wigner and pairing energies in the fragmentation potentials is discussed by considering three different temperatures, $T =$ 0.5. 1.0, and 4.1898 MeV. It is seen that for low temperatures both pairing and Wigner terms contribute significantly in the structure of the fragmentation potential. However, for the temperature corresponding to $E_{lab} = 275$ MeV for the reaction under consideration, the pairing term vanishes and the resulting structure arises only due to the Wigner term. The roles of temperature-dependent Wigner term and Wigner term at $T = 0$ MeV are also analyzed. In addition to the analysis of Wigner and pairing terms, we have also analyzed a factor α appearing in the calculation of hydrodynamical masses defining the radius of the cylinder assumed in the total nuclear volume of the two spherical fragments for the mass transfer. It is seen that this factor has a significant effect in the preformation values. For lower values of α for near symmetric

fragments, the characteristic four-nucleon structure is seen (for $\ell = 0\hbar$), which diminishes and vanishes completely with increase in α values. In general, the preformation probabilities for the fragments beyond $A_2 > 12$ increase with increase in the α values. However, this scenario changes at higher ℓ values. At higher ℓ values, for $4n$ nuclei, the preformation value is maximum for lower α value and decreases with increase in α value. However, for other fragment combinations, the preformation probability increases with increase in α values. This significant change in the preformation results also in the cross-section calculations. For different α values, the experimental data are fitted by varying the free parameter $\triangle R$ and a linear relation is obtained between $\triangle R$ and α values. Our calculated cross sections for the charge distribution of the measured fission fragments are reasonably closer to the experimental data. It is to be mentioned that exact fitting is not tried (rather it is planned) to see any correlation between only one parameter of the model, namely $\triangle R$, and the value of α (dictating the nucleon transfer in the inertia part) as a function of energy so as to make the dynamical cluster-decay model a parameter-independent model, which would account for all the fusion-fission reactions of the low-energy domain.

ACKNOWLEDGMENT

One of the authors, M.B., acknowledges financial support by the University Grants Commission of India, Grant No. 37-100/(2009).

[1] S. J. Sanders, A. Szanto de Toledo, and C. Beck, Phys. Rep. **311**, 487 (1999).
[2] N. V. Antonenko, S. P. Ivanova, R. V. Jolos, and W. Scheid, Phys. Rev. C **50**, 2063 (1994).
[3] G. G. Adamian, N. V. Antonenko, and W. Scheid, Phys. Rev. C **68**, 034601 (2003).
[4] Sh. A. Kalandarov, G. G. Adamian, N. V. Antonenko, W. Scheid, and J. P. Wieleczko, Phys. Rev. C **84**, 064601 (2011).
[5] G. Adamian, N. Antonenko, and W. Scheid, in *Clusters in Nuclei*, Lecture Notes in Physics Vol. 848, edited by C. Beck, Vol. 2 (Springer, Berlin, Heidelberg, 2012), p. 165.
[6] G. Royer, C. Bonilla, and R. A. Gherghescu, Phys. Rev. C **67**, 034315 (2003).
[7] R. A. Gherghescu and G. Royer, Phys. Rev. C **68**, 014315 (2003).
[8] R. J. Charity *et al.*, Nucl. Phys. A **476**, 516 (1988); **483**, 371 (1988).
[9] S. J. Sanders *et al.*, Phys. Rev. Lett. **59**, 2856 (1987); Phys. Rev. C **40**, 2091 (1989).
[10] T. Matsuse, C. Beck, R. Nouicer, and D. Mahboub, Phys. Rev. C **55**, 1380 (1997).
[11] R. K. Gupta, M. Balasubramaniam, C. Mazzocchi, M. La Commara, and W. Scheid, Phys. Rev. C **65**, 024601 (2002).
[12] R. K. Gupta, in *Clusters in Nuclei*, Lecture Notes in Physics Vol. 818, edited by C. Beck, Vol. 1 (Springer, Berlin, Heidelberg, 2010), p. 223.
[13] R. K. Gupta, R. Kumar, N. K. Dhiman, M. Balasubramaniam, W. Scheid, and C. Beck, Phys. Rev. C **68**, 014610 (2003).
[14] M. Balasubramaniam, R. Kumar, R. K. Gupta, C. Beck, and W. Scheid, J. Phys. G: Nucl. Part. Phys. **29**, 2703 (2003).
[15] R. K. Gupta, M. Balasubramaniam, R. Kumar, D. Singh, and C. Beck, Nucl. Phys. A **738**, 479 (2004).
[16] R. K. Gupta, M. Balasubramaniam, R. Kumar, D. Singh, C. Beck, and W. Greiner, Phys. Rev. C **71**, 014601 (2005).
[17] R. K. Gupta, M. Balasubramaniam, R. Kumar, D. Singh, S. K. Arun, and W. Greiner, J. Phys. G: Nucl. Part. Phys. **32**, 345 (2006).
[18] B. B. Singh, M. K. Sharma, and R. K. Gupta, Phys. Rev. C **77**, 054613 (2008).
[19] R. Kumar and R. K. Gupta, Phys. Rev. C **79**, 034602 (2009).
[20] R. K. Gupta, Niyti, M. Manhas, and W. Greiner, J. Phys. G: Nucl. Part. Phys. **36**, 115105 (2009).
[21] Niyti, R. K. Gupta, and W. Greiner, J. Phys. G: Nucl. Part. Phys. **37**, 115103 (2010).
[22] M. K. Sharma, G. Sawhney, R. K. Gupta, and W. Greiner, J. Phys. G: Nucl. Part. Phys. **38**, 105101 (2011).
[23] K. Sandhu, M. K. Sharma, and R. K. Gupta, Phys. Rev. C **85**, 024604 (2012).
[24] M. K. Sharma, S. Kanwar, G. Sawhney, and R. K. Gupta, Phys. Rev. C **85**, 064602 (2012).
[25] A. Ray *et al.*, Phys. Rev. C **44**, 514 (1991).
[26] C. Beck *et al.*, Phys. Rev. C **47**, 2093 (1993).
[27] S. J. Sanders, Phys. Rev. C **44**, 2676 (1991).
[28] C. Beck *et al.*, Eur. Phys. J. A **2**, 281 (1998).
[29] Sl. Cavallaro *et al.*, Phys. Rev. C **57**, 731 (1998).
[30] A. T. Hasan *et al.*, Phys. Rev. C **49**, 1031 (1994).
[31] K. A. Farrar *et al.*, Phys. Rev. C **54**, 1249 (1996).
[32] G. Rosner *et al.*, Phys. Lett. B **150**, 87 (1985).
[33] C. Karthikraj, N. S. Rajeswari, and M. Balasubramaniam, Phys. Rev. C **86**, 014613 (2012).
[34] H. J. Krappe, Phys. Rev. C **59**, 2640 (1999).
[35] C. Guet, E. Strumberger, and M. Brack, Phys. Lett. B **205**, 427 (1988).
[36] G. Audi, A. H. Wapstra, and C. Thibault, Nucl. Phys. A **729**, 337 (2003).
[37] W. D. Myers and W. J. Swiatecki, Nucl. Phys. **81**, 1 (1966).
[38] H. Kröger and W. Scheid, J. Phys. G: Nucl. Phys. **6**, L85 (1980).
[39] S. Yamaji, K. H. Ziegenhaint, H. J. Fink, W. Greiner, and W. Scheid, J. Phys. G: Nucl. Phys. **3**, 1283 (1977).
[40] N. S. Rajeswari, K. R. Vijayaraghavan, and M. Balasubramaniam, Eur. Phys. J. A **47**, 126 (2011).